Received 15 June 2020; revised 30 July 2020; accepted 9 August 2020. Date of publication 13 August 2020; date of current version 1 September 2020.

Digital Object Identifier 10.1109/OJAP.2020.3016425

Synthesis of Reflectors Characterized by the Spatial Dispersion of the Reflection Coefficient

KIRILL KLIONOVSKI [1], SERGEY E. BANKOV [2] (Member, IEEE), AND ATIF SHAMIM [1] (Senior Member, IEEE)

[1] Computer, Electrical and Mathematical Sciences and Engineering Division, King Abdullah University of Science and Technology, Thuwal 23955-6900, Saudi Arabia
[2] Kotelnikov Institute of Radio Engineering and Electronics, Russian Academy of Sciences, 125009 Moscow, Russia

CORRESPONDING AUTHORS: K. KLIONOVSKI and S. E. BANKOV (e-mail: kirill.klionovski@kaust.edu.sa; sbankov@yandex.ru)

This work was supported by King Abdullah University of Science and Technology and King Saud University Collaborative Research Grant.

ABSTRACT Planar antenna reflectors are attractive for the designs of both narrow-beam antenna arrays and frequency-scanning arrays. Planar implementation of reflectors can be performed through substrate integrated waveguide (SIW) technology. The magnitude and argument of the field reflected from such surfaces depend on the angle of the incident field. Thus, the reflector's profile should be synthesized considering the effect of spatial dispersion of the reflection coefficient to maximize the efficiency of the reflection. In this paper, we show how to synthesize a reflector's profile that is characterized by the effect of spatial dispersion of the reflection coefficient. For this purpose, we use a spectral representation of the field reflected from a surface with spatial dispersion of the reflection coefficient. Specifically, we investigate a phase error for an SIW-based parabolic reflector. We show that offset SIW-based reflectors are mostly affected by the effect of spatial dispersion of the reflection coefficient.

INDEX TERMS Reflector antenna, spatial dispersion of the reflection coefficient, surface integrated waveguide technology.

I. INTRODUCTION

THE DEVELOPMENT of modern telecommunication systems, particularly for millimeter-wave frequency bands, has resulted in the miniaturization of antennas and microwave feeding networks. One popular realization technology for such antenna systems is substrate integrated waveguide (SIW), which helps in planar implementations of traditionally nonplanar components such as waveguides and antenna reflectors. However, the reflection properties of SIW-based surfaces generally depend on the angle of incidence of an incoming wave. In this case, the effect of spatial dispersion of the reflection coefficient should be taken into account to increase the radiation efficiency of a planar antenna reflector. In classic reflectors based on metallic surfaces, the effect of spatial dispersion of the reflection coefficient is absent because coefficient's phase is constant for any incident angle [1]. In SIW-based reflectors, this effect appears due to the excitation of reactive waves near the reflection surface, which can change their structure with the variation of the incident angle. The effect of spatial dispersion of the reflection coefficient can significantly influence the reflection properties of such reflectors. Thus, typical reflectors such as those with canonical designs (i.e., parabolic, elliptic, and hyperbolic) should be corrected for this effect.

Some planar designs of SIW-based multibeam and frequency-scanning antenna arrays with reflectors have been presented in the literature [2]–[8]. In those studies, the design of an offset parabolic reflector [2], a Gregorian system [3], and a pillbox parabolic reflector [4]–[8] have been investigated. However, none of those studies have taken the effect of spatial dispersion of the reflection coefficient into account; the reflectors' profiles were chosen to be similar to that of a continuous metallic surface.

In this paper, we consider the task of synthesizing a two-dimensional (2D) reflector's profile, the surface of which is characterized by a reflection coefficient that is dependent on the incident angle of the electromagnetic waves. As particular cases of such a surface, we consider periodic gratings of circular-shaped and rectangular-shaped conductors (Fig. 1). To solve the synthesis task for the gratings, we expand the reflected field into a Fourier integral in terms of spatial harmonics, and use the reflection coefficient of the structure

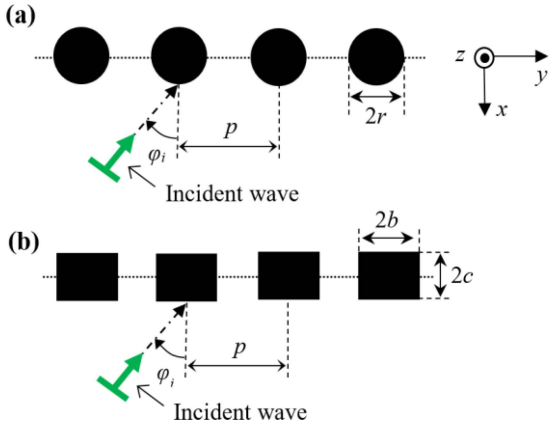

FIGURE 1. The periodic gratings of (a) circular-shaped and (b) rectangular-shaped conductors.

in the Fourier decomposition. An asymptotic representation of the Fourier integral-based reflection field is used in the synthesis procedure of a reflector profile.

II. SYNTHESIS OF THE REFLECTOR PROFILE

In this section, we derive some equations, which express a field reflected from a spatially dispersive surface through an incident field and a reflection coefficient R of the dispersive surface. We assume that R is the reflection coefficient of a plane wave from a flat surface. The results obtained in Section II-A are valid for an arbitrary reflective surface characterized by the reflection coefficient R with the dependence on the incident angle φ_i. As the particular cases of spatially dispersive surfaces, we consider the periodic gratings presented in Fig. 1.

A. REFLECTED FIELD FOR A SURFACE WITH SPATIAL DISPERSION

Let us simulate the dispersive structures, presented in Fig. 1, through a reflective plane located at $x = 0$ and characterized by the reflection coefficient R. We assume that the structure is located in a medium with a permittivity of ε. The plane is excited by the incident z-axis oriented electric field intensity vector E_z^{inc} of an arbitrary form. Then, we can write the Fourier expansion of the z-axis oriented vector E_z^{inc} in plane waves [9]:

$$E_z^{inc}(x, y) = \int_{-\infty}^{\infty} g^{inc}(\alpha) e^{i\sqrt{k^2\varepsilon - \alpha^2}x - i\alpha y} d\alpha. \quad (1)$$

Here, g^{inc} is the spatial spectrum of the incident field; $k = 2\pi/\lambda$; λ is the radiation wavelength in a vacuum; and i is the imaginary unit. We assume the time dependence in the form of $e^{i\omega T}$ (ω is angular frequency, T is time). The expansion (1) satisfies the 2D Helmholtz wave equation $\Delta E_z^{inc} + k^2 \varepsilon E_z^{inc} = 0$ in the medium with the permittivity of ε. Each partial plane wave in (1) can also be characterized by the angle of incidence φ_i, which corresponds to the spectral parameter α as follows:

$$\alpha = k\sqrt{\varepsilon} \sin \varphi_i. \quad (2)$$

Each partial plane wave from (1) is reflected from the surface with the reflection coefficient $R(\alpha)$. Then, the reflected field has the following form:

$$E_z^{refl}(x, y) = \int_{-\infty}^{\infty} g^{inc}(\alpha) R(\alpha) e^{-i\sqrt{k^2\varepsilon - \alpha^2}x - i\alpha y} d\alpha. \quad (3)$$

At the plane of $x = 0$, we can represent the spectrum of the incident field using the inverse Fourier transform of the incident field, as shown in (3):

$$g^{inc}(\alpha) = \frac{1}{2\pi} \int_{-\infty}^{\infty} E_z^{inc}(0, y') e^{i\alpha y'} dy'. \quad (4)$$

Then, the reflected field at plane $x = 0$ has the following integral representation after (4) is substituted into (3):

$$E_z^{refl}(y) = \int_{-\infty}^{\infty} E_z^{inc}(0, y') G(y - y') dy',$$
$$G(y - y') = \frac{1}{2\pi} \int_{-\infty}^{\infty} R(\alpha) e^{-i\alpha(y - y')} d\alpha. \quad (5)$$

Equation (5) describes a non-local coupling between the reflected and incident fields because the reflected field at the point y depends on the incident field at the point y'. The variable y' is varied from minus to plus infinity. If the coupling is absent, we can see that the function $G(y)$ becomes the Dirac delta function, and the reflected field is determined through the incident field by the geometrical optics (GO) laws in the case where the reflection coefficient does not depend on the parameter α and, thus, the angle of incidence φ_i. In the case where the spatial dispersion of the reflection coefficient exists, the dependence R on the incident angle φ_i influences the reflected field, and expression (5) describes the general relation between the incident and reflected fields. For the gratings presented in Fig. 1, it will be shown in the following sections that the function $G(y)$ is localized in some vicinity of the point $y = 0$. It has a maximum at $y = 0$ and decreases rapidly when moving away from this point. The localization of the function $G(y)$ means that the speed of changing of R from the incident angle φ_i is not very high. Notably, because of the reciprocity of the structure, the reflection coefficient $R(\alpha)$ and therefore function $G(y)$ are even functions of their arguments.

Let us consider a curved reflector (Fig. 2). If the radius of the reflector bending is large, (5) can be written in the local curved orthogonal coordinate system nsz (n is normal to the illuminated surface) as follows:

$$E_z^{refl}(s) = \int_{-\infty}^{\infty} E_z^{inc}(s') G(s - s') ds'. \quad (6)$$

Let us write the incident field through its magnitude and argument as $E_z^{inc}(s') = |E_z^{inc}(s')| \exp(i\varphi^{inc}(s'))$. On the surfaces of quasioptical reflectors, as a rule, the magnitude of the incident field changes much more slowly than the argument does. Therefore, we can consider the magnitude to be a constant $|E_z^{inc}(s')| = |E_z^{inc}(s)|$. With the assumption of the slow changing of the magnitude of the incident field, we

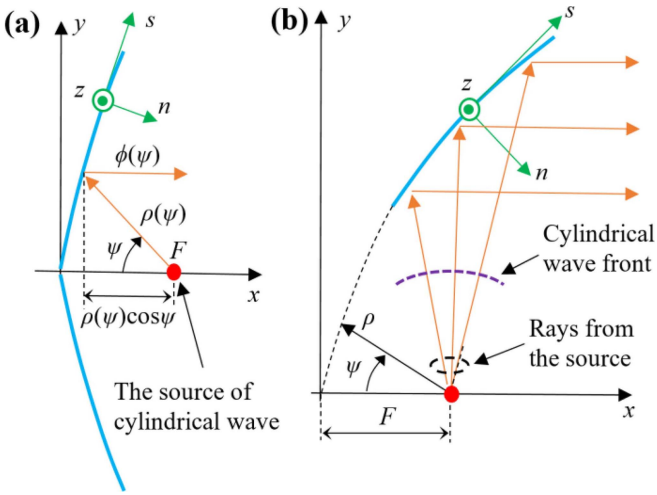

FIGURE 2. (a) Symmetric and (b) offset reflector excited by the source of the cylindrical wave.

can write (6) as follows:

$$E_z^{refl}(s) = \left|E_z^{inc}(s)\right| \int_{-\infty}^{\infty} e^{i\varphi(s')} G(s-s')ds'. \tag{7}$$

Let us consider a case where function $G(s-s')$ is an even one and it is localized near point $s = s'$. Such behavior of the integral core allows us to expand the phase of the incident wave through a Taylor series expansion, which contains only the first three terms of the expansion:

$$\varphi(s') = \varphi(s) + (s'-s)\frac{d\varphi(s)}{ds} + \frac{(s'-s)^2}{2}\frac{d^2\varphi(s)}{ds^2}. \tag{8}$$

Substituting (8) into (7) with the changing of variables $t = s' - s$ gives us the following form of the reflected field:

$$\begin{aligned} E_z^{refl}(s) &= \left|E_z^{inc}(s)\right| e^{i\varphi(s)} \int_{-\infty}^{\infty} e^{-itk_\tau} e^{it^2\varphi''} G(t)dt \\ &= E_z^{inc}(s) \int_{-\infty}^{\infty} e^{-itk_\tau} e^{it^2\varphi''} G(t)dt. \end{aligned} \tag{9}$$

Here, we denote $k_\tau = -d\varphi(s)/ds$, where k_τ is associated with the tangential component of the GO ray incident on the reflector at point s, and $\varphi'' = d^2\varphi(s)/2ds^2$. The second exponent in (9) can be represented through the following Taylor series:

$$e^{it^2\varphi''} = \sum_{n=0}^{\infty} \frac{(i\varphi'')^n t^{2n}}{n!}. \tag{10}$$

The multiplier -*it* in (10) is equivalent to derivative $\partial/\partial k_\tau$. Thus, the integral in (9) can be presented using (10) as follows:

$$\int_{-\infty}^{\infty} e^{-itk_\tau} t^{2n} G(t)dt = \begin{cases} i^{2n}\frac{\partial^{2n}}{\partial k_\tau^{2n}} \int_{-\infty}^{\infty} e^{-itk_\tau} G(t)dt, & n \neq 0, \\ \int_{-\infty}^{\infty} e^{-itk_\tau} G(t)dt, & n = 0. \end{cases} \tag{11}$$

The zeroth term in (11) is the reflection coefficient $R(k_\tau)$ in accordance with (5):

$$\int_{-\infty}^{\infty} e^{-itk_\tau} G(t)dt = R(k_\tau). \tag{12}$$

Then, the reflected field has the following form after (11) is substituted into (9):

$$E_z^{refl}(s) = E_z^{inc}(s)\left(R(k_\tau) + \sum_{n=1}^{\infty} \frac{(-i\varphi'')^n}{n!} \frac{\partial^{2n} R(k_\tau)}{\partial k_\tau^{2n}}\right). \tag{13}$$

Here, the first term corresponds to the GO field, where the incident field multiplies with the reflection coefficient $R(k_\tau)$. The amendment to the GO reflected field is described through the sum containing the derivatives from the reflection coefficient. The multiplier in the brackets (13) can be considered as a generalized reflection coefficient.

B. THE REFLECTOR'S PROFILE

Let us synthesize the profile of the reflector characterized by the reflection coefficient R. The profile of the reflector is determined through the function $\rho(\psi)$ for $\psi \in [-\psi_{\max}, \psi_{\max}]$. The focal point $x = F$ is the point of convergence of the rays reflected from the reflector when a plane wave propagating along the x-axis is incident on the reflector (Fig. 2). We assume that a point source of a cylindrical wave exists in the focal point. Then, the phase condition of the transformation of the cylindrical wave front into a plane wave front after the reflection from the reflector in the GO approximation (Fig. 2(a)) is as follows:

$$k\sqrt{\varepsilon}\rho(\psi) - \phi(\psi) = k\sqrt{\varepsilon}F - \phi(0) + k\sqrt{\varepsilon}(F - \rho(\psi)\cos\psi). \tag{14}$$

Here, the term $\phi(\psi)$ describes the dependence of the phase of the reflected ray on the incident angle. This term is the argument of the generalized reflection coefficient. For the case when G is a localized function, the term $\phi(\psi)$ is found from the formula (13):

$$\phi(\psi) = \arg\left(R(k_\tau(\psi)) + \sum_{n=1}^{\infty} \frac{(-i\varphi'')^n}{n!} \frac{\partial^{2n} R(k_\tau(\psi))}{\partial (k_\tau(\psi))^{2n}}\right). \tag{15}$$

The parameter $k_\tau(\psi)$ is expressed through the function $\rho(\psi)$ as follows (see Appendix):

$$k_\tau(\psi) = \frac{\rho'(\psi)}{\sqrt{(\rho'(\psi))^2 + \rho(\psi)^2}}, \tag{16}$$

where $\rho'(\psi) = d\rho(\psi)/d\psi$. The reflector's profile is determined using (14) as follows:

$$\rho(\psi) = \frac{2Fk\sqrt{\varepsilon} + \phi(\psi) - \phi(0)}{k\sqrt{\varepsilon}(1+\cos\psi)}. \tag{17}$$

In the case of the effect of spatial dispersion of the reflection coefficient being absent (when $\phi(\psi) = \phi(0)$), (17) describes the shape of the parabolic reflector: $\rho(\psi) = 2F/(1+\cos\psi)$. In a general case, formula (17) is a nonlinear differential equation because phase $\phi(\psi)$ depends on the $\rho(\psi)$ and its first derivative. This equation should be solved numerically.

The area of application of the presented synthesis procedure is limited by the condition of localization of the function $G(s)$. If the function $G(s)$ is not localized, which corresponds to very high speed of changing of R from the incident angle φ_i, then the simple representation of the argument of the generalized reflection coefficient through the sum (15) gives low accuracy of the determination of $\phi(\psi)$. For the case of a non-localized function $G(s)$, we should find $\phi(\psi)$ using the general integral representation of the reflected field (6). It should be noted that surfaces, which are interesting from a practical realization point of view, do not have such a strong dispersion that interrupts the localization of the function $G(s)$.

III. ANALYSIS OF THE REFLECTIVE SURFACES

We consider the 2D periodic gratings of circular-shaped and rectangular-shaped conductors (Fig. 1) located in a medium with a permittivity of ε. The period of the gratings is p. The radius of the circular-shaped conductors is r. The dimension of the rectangular-shaped conductors is $2b$ and $2c$ along the y and x-axis, respectively. A plane wave is incident on the gratings at angle φ_i. The electric field intensity vector $\mathbf{E}$ of the incident wave is oriented along the z-axis. The reflection properties of the considered gratings have been studied in [10]–[14]. Some analytical formulae of the reflection coefficient, when the radius of the circular-shaped conductors is much smaller than period $r << p$, are available in [10], [12], [14]. Some analytical formulae of the reflection coefficient for the grating of rectangular-shaped conductors are available in [13], [14]. Furthermore, [11] provides some analytical formulae of the reflection coefficient for the problem of plane wave diffraction by an arbitrary-shaped small period grating. In this paper, we use the following formula of the reflection coefficient of the plane wave from the gratings determined through the fill factor $q = 2r/p$ or $q = 2b/p$, [13]:

$$R = \frac{1 + ik\sqrt{\varepsilon}pl_1 \cos\varphi_i}{2 - 2ik\sqrt{\varepsilon}pl_1 \cos\varphi_i} + \frac{1 + ik\sqrt{\varepsilon}pl_2 \cos\varphi_i}{2 - 2ik\sqrt{\varepsilon}pl_2 \cos\varphi_i}. \quad (18)$$

For the circular-shaped conductors grating, the parameters l_1 and l_2 are determined as follows:

$$\begin{aligned} l_1 &= \pi\nu q^2/(2l_3) - (1/\pi)\ln(\cosh l_4), \\ l_2 &= \pi\nu q^2/(2l_3) - (1/\pi)\ln(\sinh l_4), \\ l_3 &= \ln(\sin((1+\nu)\pi q/2)/\sin((1-\nu)\pi q/2)), \\ l_4 &= \pi q/2 + (\pi q/l_3)\arctan(\tan(\pi q\nu/2)\cot(\pi q/2)), \end{aligned} \quad (19)$$

where ν is determined through the following non-linear equation:

$$\pi q \sin(\pi q\nu) = 2\Big(\sinh^2(\pi q/2) + \sin^2(\pi q\nu/2)\Big)l_3.$$

For the rectangular-shaped conductors grating, the parameters l_1 and l_2 are determined as follows:

$$\begin{aligned} l_1 &= l_3 - \ln((\sigma-1)/\sigma)/(2\pi), \\ l_2 &= l_3 + \ln(\sigma-1)/(2\pi), \end{aligned} \quad (20)$$

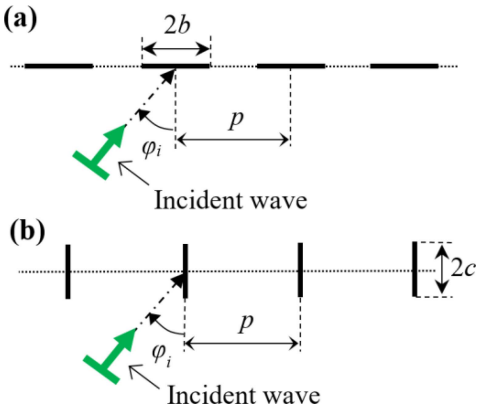

FIGURE 3. The periodic gratings of (a) horizontal and (b) vertical strip conductors.

where l_3 and σ are determined through a complex system of integral equations [13]. For the particular case of the horizontal strip conductors (Fig. 3(a)) when $c \to 0$, formula (18) can be simplified as follows:

$$R = -\frac{1}{2} - \frac{1 - (1/\pi)ik\sqrt{\varepsilon}p\ln(1/\sin(\pi q/2))\cos\varphi_i}{2 + (1/\pi)2ik\sqrt{\varepsilon}p\ln(1/\sin(\pi q/2))\cos\varphi_i}. \quad (21)$$

For the particular case of the vertical strip conductors (Fig. 3(b)) when $b \to 0$, formula (18) can be simplified as follows:

$$\begin{aligned} R = &\frac{-1 + (1/\pi)ik\sqrt{\varepsilon}p\cos\varphi_i\ln(\cosh(\pi c/p))}{2 + (1/\pi)2ik\sqrt{\varepsilon}p\cos\varphi_i\ln(\cosh(\pi c/p))} \\ &- \frac{1 - (1/\pi)ik\sqrt{\varepsilon}p\cos\varphi_i\ln(\sinh(\pi c/p))}{2 + (1/\pi)2ik\sqrt{\varepsilon}p\cos\varphi_i\ln(\sinh(\pi c/p))}. \end{aligned} \quad (22)$$

Note that formulae (18), (21) and (22) were obtained with the assumption that $p << \lambda/\sqrt{\varepsilon}$. However, they allow the calculation of the reflection coefficient precisely for p up to $\lambda/(4\sqrt{\varepsilon})$.

Fig. 4 presents the dependence of the magnitude of the reflection coefficient on the fill factor or the ratio $2c/p$ for different angles of incidence of the plane wave. These figures show that the magnitude of the reflection coefficient is practically equal to 1 for any angle φ_i when the fill factor is greater than 0.2 and 0.6 for the circular-shaped and horizontal strip conductors, respectively. Fig. 4(c) shows that even for the normal wave incidence when $\varphi_i = 0$, there is a full wave reflection from the infinite thin vertical strips of the dimension $2c/p > 0.7$. Thus, any of the presented structures can be used as the surface of a reflector.

Fig. 5 presents the dependence of the argument of the reflection coefficient on the incident angle for different fill factors or the ratios $2c/p$. These figures show that the argument of the reflection coefficient changes for different incident angles. The effect of spatial dispersion of the reflection coefficient exists for all of the considered gratings. The highest speed of changing of the argument of the reflection coefficient from the incident angle appears mostly for the circular shaped wire grating when $q = 0.4$ and 0.6. Therefore, the difference between the profile synthesized by formula (17) is most strongly different from the parabolic one at the indicated fill factor values.

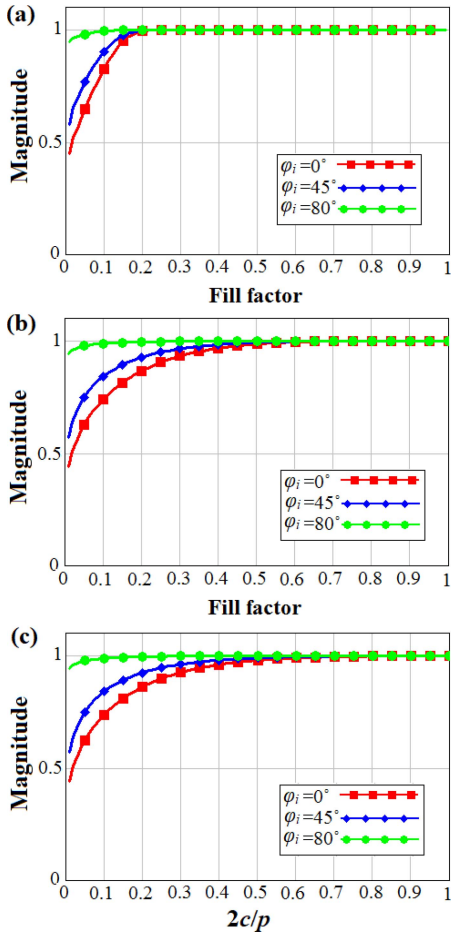

FIGURE 4. The dependence of magnitude of R on the fill factor (or the ratio $2c/p$) and the angle of incidence for (a) the circular-shaped, (b) horizontal strip, and (c) vertical strip conductors when $p = 0.1\lambda$ and $\varepsilon = 6$.

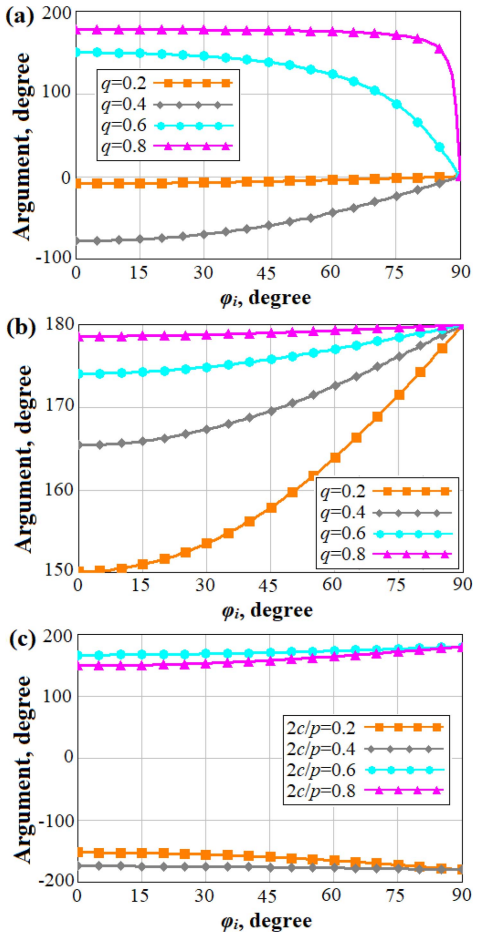

FIGURE 5. The dependence of argument of R on the fill factor (or the ratio $2c/p$) and the angle of incidence for (a) the circular-shaped, (b) horizontal strip, and (c) vertical strip conductors when $p = 0.1\lambda$ and $\varepsilon = 6$.

IV. NUMERICAL RESULTS

Let us synthesize the reflector's profile for a practical case when a symmetric or an offset reflector is excited by a SIW-implemented horn (Fig. 6). We assume that the phase center of the horn is located at the focal point, and the parameters of the SIW-based reflector's surface are the following: $q = 0.4$ and 0.6, $p = 0.1\lambda$, and $\varepsilon = 6$. We assume that the focal distance of the reflector is $F = 8\lambda$ and the maximum flare angle is $\psi_{\max} = 120°$. Such a flare angle allows us to analyze both the symmetric and offset reflectors in one figure.

Let us firstly analyze the function $G(s)$ for the circular-shaped grating using the spectral representation (5). We assume that the spectrum in (5) is limited by the following interval: $|\alpha| < k\sqrt{\varepsilon}$. This means that we do not take into account the contribution of the decaying reactive waves created by the source. Such a limitation can be justified because at the considered reflector systems, the distance between the source and reflector surface is usually large, and the contribution of reactive components is negligible. Fig. 7 plots the normalized function $|G(s)/G(0)|$ for $q = 0.4$ and 0.6. This figure shows that the function $G(s)$ is localized near point $s = 0$. Therefore, we can apply formula (13)

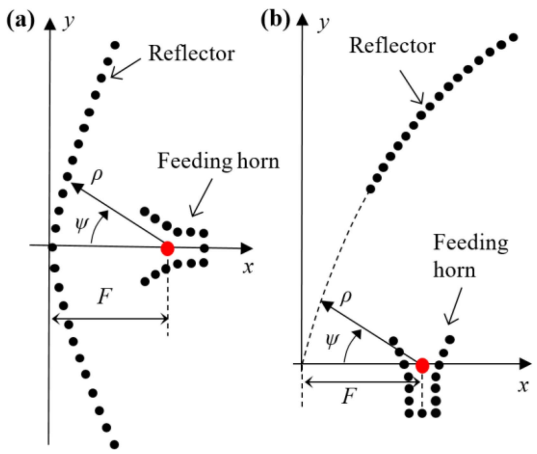

FIGURE 6. (a) Symmetric and (b) offset SIW-based reflector excited by the SIW-implemented horn.

for the analysis of the field reflected from the SIW-based surface, and formula (17) for the synthesis of the reflector's profile. Figure 8 shows a synthesized profile for the SIW-based reflector as compared to a parabolic one, as well as the difference between synthesized and parabolic curves.

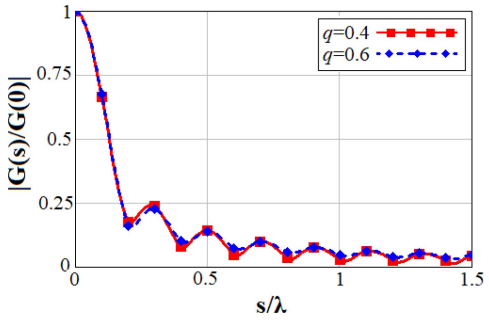

FIGURE 7. Normalized magnitude of $G(s)$ when $p = 0.1\lambda$ and $\varepsilon = 6$.

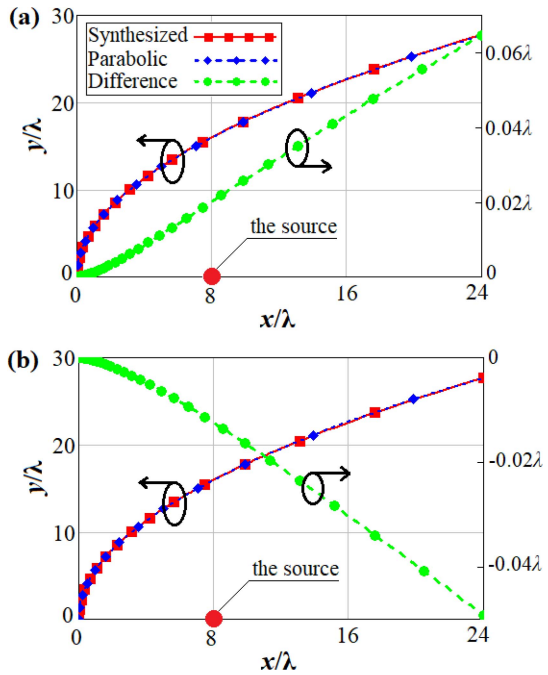

FIGURE 8. Synthesized and parabolic profiles for (a) $q = 0.4$ and (b) $q = 0.6$.

We can see from this figure that the main difference of $0.05\lambda - 0.065\lambda$ is observed at the edge of the reflector. Let us plot Fig. 9 with the dependence of a phase error, which is created by the parabolic profile made of SIW-based surface. As we can see from Fig. 9, the phase error of more than 10° is observed for $y > 10\lambda$ when $q = 0.4$, which corresponds to the angles $\psi > 50°$. Therefore, the effect of spatial dispersion of the reflection coefficient affects mostly offset reflectors.

Let us investigate the dependence of the phase error on the reflector's curvature. The curvature can be changed by changing the focal distance F. It is determined through formula (17), which can be represented as follows:

$$\rho(\psi) = \frac{2F}{1+\cos\psi} + \frac{\phi(\psi) - \phi(0)}{k\sqrt{\varepsilon}(1+\cos\psi)}. \qquad (23)$$

Here, the first term is the parabolic shape. The second term represents the amendment to the original parabolic shape, and it takes into account the effect of spatial dispersion of the reflection coefficient. The second term determines the phase

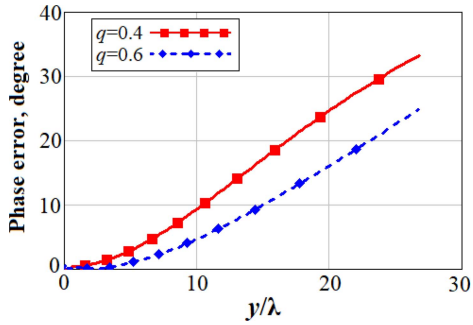

FIGURE 9. Phase error versus the y-coordinate of the parabolic reflector.

error, and it can be noted that it contains the argument of the generalized reflection coefficient, which does not depend on F. Therefore, the change of the reflector's curvature does not influence the phase error.

It can be shown that the influence of spatial dispersion of reflection coefficient is increasing with the increase in the period p. Therefore, the influence of effect will be stronger for millimeter wave antenna reflectors when there is a technological limitation on the minimum period fabrication.

Note also that, in general, metamaterial-based surfaces are characterized by the effect of spatial dispersion of the reflection coefficient [15]. Therefore, the presented synthesis procedure is applicable to metamaterial-based parabolic reflectors.

V. CONCLUSION

In this paper, we considered the problem of synthesis of a reflector's profile for the case when its surface is characterized by the spatial dispersion of reflection coefficient. We derived a spectral representation of the field reflected from such surface, which is used for the synthesis procedure. We investigated the applicability of the spectral representation for synthesis of the SIW-based reflectors. We showed that the effect of spatial dispersion of the reflection coefficient affects mostly offset SIW-based reflectors. This effect may produce sufficient phase error that should be taken into account in the reflector synthesis.

APPENDIX

Let us find the component k_τ, which is associated with the tangential component of the GO ray incident on the reflector at point A from focal point F (Fig. A1). Vector $\mathbf{k}$, which is directed along the direction of propagation of the GO ray, has the following representation in the Cartesian coordinates (x, y) : $\mathbf{k} = (-\cos\psi, \sin\psi)$. Vector $\boldsymbol{\tau}$, which is tangential to the reflector at point A, is expressed through the angle γ as follows: $\boldsymbol{\tau} = (\cos\gamma, \sin\gamma)$. Parameter k_τ is the projection of the vector $\mathbf{k}$ on the vector $\boldsymbol{\tau}$: $k_\tau = (\mathbf{k}\cdot\boldsymbol{\tau}) = -\cos(\psi+\gamma)$. Let us express k_τ through the radius ρ. For this purpose, we consider an infinitely small angle $d\psi \to 0$ (Fig. A1). Radius $\rho + \rho' d\psi$, where $\rho' = d\rho/d\psi$, corresponds to the angle $\psi + d\psi$. Taking into account the condition of $d\psi \to 0$, we can find angle γ as follows: $\gamma =$

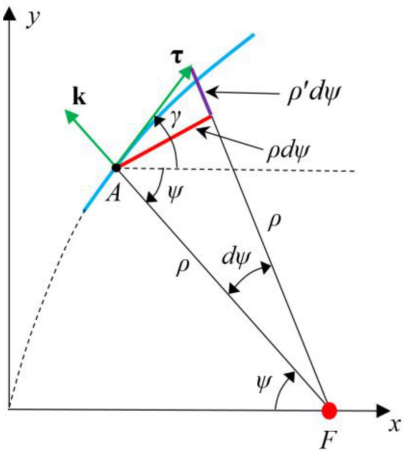

FIGURE A1. The determination of the component k_τ.

$\pi/2-\psi+\arctan(\rho'/\rho)$, and the parameter k_τ is expressed as follows: $k_\tau = \sin(\arctan(\rho/\rho'))$. Applying some trigonometric conversions for "sin" and "arctan" functions, we obtain the following representation of k_τ:

$$k_\tau = \frac{\rho'}{\sqrt{\rho'^2+\rho^2}}. \tag{A.1}$$

REFERENCES

[1] S. Cornbleet, *Microwave Optics: The Optics of Microwave Antenna Design*. London, U.K.: Academic, 1976.
[2] Y. J. Cheng, W. Hong, and K. Wu, "Millimeter-wave substrate integrated waveguide multibeam antenna based on the parabolic reflector principle," *IEEE Trans. Antennas Propag.*, vol. 56, no. 9, pp. 3055–3058, Sep. 2008.
[3] M. Ettorre, A. Neto, G. Gerini, and S. Maci, "Leaky-wave slot array antenna fed by a dual reflector system," *IEEE Trans. Antennas Propag.*, vol. 56, no. 10, pp. 3143–3149, Oct. 2008.
[4] M. Ettorre, R. Sauleau, L. Le Coq, and F. Bodereau, "Single-folded leaky-wave antennas for automotive radars at 77 GHz," *IEEE Antennas Wireless Propag. Lett.*, vol. 9, pp. 859–862, 2010.
[5] M. Ettorre, R. Sauleau, and L. Le Coq, "Multi-beam multi-layer leaky-wave SIW pillbox antenna for millimeter-wave applications," *IEEE Trans. Antennas Propag.*, vol. 59, no. 4, pp. 1093–1100, Apr. 2011.
[6] E. Gandini, M. Ettorre, M. Casaletti, K. Tekkouk, L. Le Coq, and R. Sauleau, "SIW slotted waveguide array with pillbox transition for mechanical beam scanning," *IEEE Antennas Wireless Propag. Lett.*, vol. 11, pp. 1572–1575, 2012.
[7] S. E. Bankov, G. G. Grachev, M. D. Duplenkova, and E. V. Frolova, "Design and experimental investigation of a multibeam integrated reflector antenna of the millimeter wave band," *J. Commun. Technol. Electron.*, vol. 59, no. 6, pp. 504–522, Jun. 2014.
[8] S. E. Bankov and E. V. Frolova, "Design and experimental study of a planar multibeam double-reflector aplanatic system," *J. Commun. Technol. Electron.*, vol. 62, no. 5, pp. 489–495, May 2017.
[9] L. B. Felsen and N. Marcuvitz, *Radiation and Scattering of Waves*. Hoboken, NJ, USA: Wiley, 2003.
[10] J. R. Wait, "Reflection at arbitrary incidence from a parallel wire grid," *Appl. Sci. Res.*, vol. 4, pp. 393–400, Dec. 1955.
[11] V. M. Astapenko and G. D. Malyuzhinets, "Diffraction of a plane wave by a partial periodic grating," *Soviet Phys. Acoust. Engl. Transl.*, vol. 16, no. 3, pp. 299–305, 1970.
[12] G. Z. Aizenberg, V. G. Yampol'skii, and O. N. Tereshin, *Ultrashort-Wave Antennas. Part 2*. Moscow, Russia: Svyaz', 1977.
[13] E. I. Nefedov and A. N. Sivov, *Electrodynamics of Periodical Structures*. Moscow, Russia: Nauka, 1977.
[14] V. P. Shestopalov *et al.*, *Resonant Scattering of Waves. Diffraction Gratings. Part 1*. Kyiv, Ukraine: Naukova Dumka, 1986.
[15] V. S. Asadchy, M. Albooyeh, S. N. Tcvetkova, A. Díaz-Rubio, Y. Ra'Di, and S. A. Tretyakov, "Perfect control of reflection and refraction using spatially dispersive metasurfaces," *Phys. Rev. B*, vol. 94, no. 7, pp. 1–14, 2016.

KIRILL KLIONOVSKI was born in Krasnogorsk, Russia. He received the Engineering degree (Hons.) in electrical engineering from Moscow Aviation Institute, Moscow, Russia, in 2010, and the Ph.D. degree in radiophysics from the Kotel'nikov Institute of Radioengineering and Electronics, Russian Academy of Sciences, Moscow, in 2015.

His current research interests include rigorous and asymptotic methods in applied electromagnetics and reflector antennas.

SERGEY E. BANKOV (Member, IEEE) was born in Stavropol City, Russia, in 1958. He received the M.S. degree in radio engineering from Moscow Power Engineering Institute (MPEI) in 1981, and the Ph.D. and Doctor of Science degrees in antenna and microwave engineering from MPEI, Moscow, in 1986 and 1994, respectively.

From 1981 to 1991, he was an Engineer and a Researcher with the Millimeter Wave Laboratory, Radio Engineering Department, MPEI. Since 1992, he was an Assistant Professor and a Professor with Radio Engineering Department, MPEI. From 1996 to 1998, he was a Visiting Researcher with Samsung El. Company, Seoul, South Korea. From 1999, he is a Chief Researcher with Kotel'nikov Institute of Radioengineering and Electronics, Russian Academy of Sciences. He has authored 14 books, more than 250 articles, and 25 patented inventions. His research interests include electromagnetic theory, antenna theory and design, microwave engineering, and metamaterials.

Dr. Bankov is an Associate Editor of the *Journal of Communications Technology and Electronics* and the *Journal of Radio Electronics*. He is a member of Russian Academy of Electrical Science and the Chair of IEEE Russia Section.

ATIF SHAMIM (Senior Member, IEEE) received the M.S. and Ph.D. degrees in electrical engineering from Carleton University, Canada, in 2004 and 2009, respectively, where he was an NSERC Alexander Graham Bell Graduate Scholar from 2007 till 2009, and an NSERC Postdoctoral Fellow from 2009 to 2010 with Royal Military College Canada and KAUST. In August 2010, he joined the Electrical Engineering Program with KAUST, where he is currently an Associate Professor and a Principal Investigator with IMPACT Lab. He was an Invited Researcher with the VTT Micro-Modules Research Center, Oulu, Finland, in 2006. His research work has won best paper awards in IEEE EuWiT 2008, IEEE IMS 2016, IEEE MECAP 2016, First Prize in IEEE IMS 2019 3MT competition and finalist/honorable mention prizes in IEEE APS Design Competition 2020, IEEE APS 2005, IEEE IWAT 2006, IEEE IMS 2014, IEEE IMS 2017 (3MT competition). He was given the Ottawa Centre of Research Innovation (OCRI) Researcher of the Year Award in 2008 in Canada. He has authored/coauthored 250 international publications, an inventor on 25 patents and has given over 50 invited talks at various international forums. His research interests are in innovative antenna designs and their integration strategies with circuits and sensors for flexible and wearable wireless sensing systems through a combination of CMOS and additive manufacturing technologies. His work on Wireless Dosimeter won the ITAC SMC Award at Canadian Microelectronics Corporation TEXPO in 2007. He is also won numerous business-related awards, including the 1st Prize in Canada's National Business Plan Competition and was awarded the OCRI Entrepreneur of the Year Award in 2010. He served on the editorial board of the IEEE TRANSACTIONS ON ANTENNAS AND PROPAGATION from 2013 to 2019, and as a Guest Editor for IEEE ANTENNAS AND WIRELESS PROPAGATION LETTERS Special issue in 2019, and is currently serving as an Associate Editor for the IEEE JOURNAL OF ELECTROMAGNETICS, RF AND MICROWAVES IN MEDICINE AND BIOLOGY.